Role of the Fermi Surface in Adsorbate−Metal Interactions: An Energy Decomposition Analysis

P. H. T. Philipsen and E. J. Baerends*

Department of Chemistry, Section Theoretical Chemistry, Vrije Universiteit, Amsterdam, De Boelelaan 1083, 1081 HV Amsterdam, The Netherlands

Received: February 10, 2006; In Final Form: April 21, 2006

We present the result of a fragment-based energy decomposition analysis on some molecule−surface interactions. The analysis allows us to quantify the Pauli repulsion, its relief, and the attractive orbital interaction energy. In a metal, the existence of incompletely occupied energy bands causes significant relief of the Pauli repulsion due to escape of antibonding electrons to unoccupied states at the Fermi energy. This is the key electronic structure feature of metals that causes metal−molecule bond energies to be stronger and dissociation barriers of chemisorbed molecules to be much lower than those in comparable systems with no or one metal atom. As examples, we discuss the energy decomposition for the activated dissociation of hydrogen on the Cu surface and its unactivated dissociation on Pd, and for the (activated) chemisorption of N_2 on W. We show that in all cases the relief of Pauli repulsion is of crucial importance for the chemisorption energy and for the low (or nonexistent) dissociation barriers. The barrier to the chemisorption well for nitrogen on tungsten is clearly related to a late relief of the Pauli repulsion. The relief of Pauli repulsion is important in lowering the barrier to dissociation of H_2 on both Cu and Pd, but the difference in barrier heights for Cu and Pd appears to not be due to stronger relief of Pauli repulsion on Pd but primarily to the Pauli repulsion itself being stronger on Cu than on Pd, the relief energy being quite comparable on the two metals.

1. Introduction

In the second half of the last century, the molecular orbital (MO)-based interpretation of chemical bonding between molecular fragments has been extensively developed. The qualitative MO (QMO) theory, usually denoted as frontier orbital theory or perturbative MO (PMO) theory, has greatly enhanced our insight into chemical bonding and has been codified in several excellent textbooks.[1−6] Concepts stemming from the QMO theory have been quantified in energy decomposition schemes. The one introduced by Morokuma[7−9] for Hartree−Fock wave functions has been used widely. It quantifies notions such as exchange repulsion or Pauli repulsion (occupied−occupied orbital interaction), which is a very general concept that plays a role in many different many-Fermion systems.[10] Other energy terms are electrostatic interaction (Coulomb interaction between the charge distributions of unmodified fragments) and occupied−virtual orbital interaction (charge transfer and polarization). We refer to ref 11 for a recent review of the concepts and insight that such a decomposition affords in the role of the kinetic energy, charge shifts, and potential energy terms in the phenomenon of chemical bonding.

Basically, the same notions as those used for isolated molecules apply to the case of bonding and reactivity of molecules with metallic surfaces. The QMO approach to bonding in solids is discussed in textbooks, for example, refs 3 and 12, while a lucid account of molecule−surface interactions has been given in a little book by Hoffmann.[13] Of course the replacement, in a one-electron picture, of the discrete levels in molecules by bands of one-electron levels in solids makes an important difference. In metals, a key element is the existence of a Fermi surface. It has often been noted that this electronic structure feature makes a difference for the Pauli repulsion component of the interaction. The Pauli repulsion arises in its most general formulation from the necessary antisymmetrization requirement on wave functions. It is customary to construct as a first step in the interaction between two systems *A* and *B* with wave functions Ψ_A and Ψ_B a zero-order wave function, Ψ^0, in which only the Pauli exclusion principle is enforced by antisymmetrization ($\hat{A}$) and renormalization (N) of the product function $\Psi_A\Psi_B$

$$\Psi^0 = N\hat{A}\{\Psi_A\Psi_B\} \tag{1}$$

The wave function Ψ^0 embodies changes in kinetic energy and in electronic density compared to the isolated systems. The net effect is that the rise in kinetic energy outweighs the attractive Coulombic energy terms, hence repulsion.[11] Note that eq 1 is a general expression that can also be applied to correlated wave functions. In an orbital model of interaction between two fully occupied MOs on fragments *A* and *B*, the repulsion is depicted as a stronger rise in the orbital energy of the antibonding orbital compared to the energy lowering of the bonding one. In Figure 1, the orbital interaction diagram is drawn of the prototype forbidden reaction of two H_2 molecules, or an H_2 molecule and a metal dimer M_2 with an s−s bonding orbital, the two systems approaching side-on to go through a square-planar transition state in the process of breaking the existing bonds between atoms 1 and 2 and 3 and 4 and forming two new bonds between atoms 1 and 3 and atoms 2 and 4. The initial repulsion accounting for the existence of the reaction barrier is the Pauli repulsion of the electron pairs in the bonding orbitals of *A* and *B*, *Ab* and *Bb*. The repulsion is embodied in the rising antibonding combination 1*a*. Only when this level approaches the unoccupied

* Corresponding author. E-mail: ej.baerends@few.vu.nl.

10.1021/jp060886e CCC: $33.50
Published on Web 06/03/2006

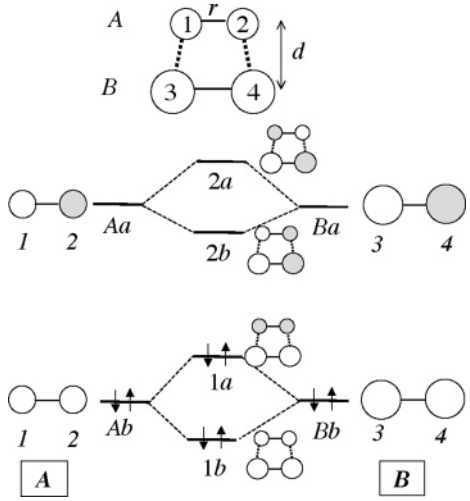

Figure 1. Orbital interaction diagram for side-on approach of two *s*-bonded dimers, for example, H_2 (*A*) and a metal dimer M_2 (*B*).

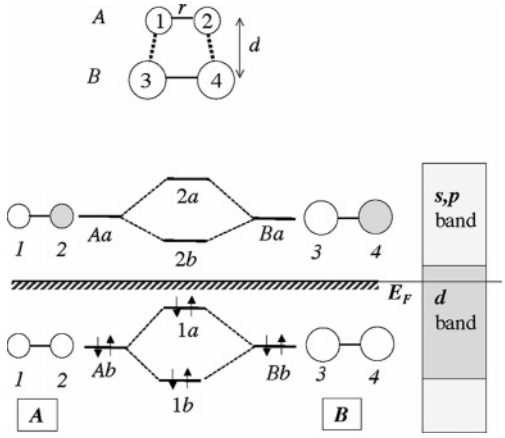

Figure 2. Orbital interaction diagram between the occupied and virtual molecular orbitals and metal *s* orbitals (two metal atoms in the unit cell) at some **k** point. The presence of the Fermi level is indicated, as well as, to the right, the presence of *s*, *p*, and *d* bands.

2*b* level, the repulsion can be diminished, first by configuration mixing between the configurations $|(1b)^2(1a)^2|$ and $|(1b)^2(2b)^2|$, and upon closer approach by transferring the antibonding electrons in 1*a* almost fully to the by then lower level 2*b*. This is the prototype of a forbidden reaction, where the virtual levels by symmetry do not mix with the occupied levels, so there is no reduction in the energy of the rising level 1*a* due to such a favorable interaction, and the antibonding 1*a* has to rise all the way up to meet some virtual level (in our case 2*b*). This picture uses the Hartree−Fock molecular orbital model plus CI. In the case of Kohn−Sham calculations, it is well-known that this particular molecular orbital model uses a single determinantal wave function, with the orbitals occupied according to the Aufbau principle, to describe the model system of noninteracting electrons. The requirement of an Aufbau configuration for the single determinant method of Kohn−Sham seems to imply that there should be an abrupt change of configuration $D_1 = |(1b)^2(1a)^2|$ to $D_2 = |(1b)^2(2b)^2|$. However, this is not the case. There will actually be a distance region $d_1 < d < d_2$ where the KS orbital energies of 1*a* and 2*b* are equal, and the density that is described in conventional CI calculations by a strong mixing of the two configurations is described in the Kohn−Sham model by an ensemble density $\rho = (1 - \omega)\rho(D_1) + \omega\rho(D_2)$, $0 \leq \omega \leq 1$, see ref 14 for details.

If system *A* does not interact with molecule *B* with discrete levels, but with metal *B*, we may use the orbital *Bb* as representative of the metallic states with which the MO *Ab* will interact most strongly, see Figure 2. Actually, if we deal with only *s* states on the metal atoms, and two metal atoms per two-dimensional unit cell, there will be at each **k** point just the same four-orbital interaction diagram. There is, however, the very important difference that now there is a Fermi energy, and the repulsive force will be lost as soon as level 1*a* rises above the Fermi energy, so that it can shed its electrons to the levels at E_F, at other **k** points. It will be all-important what the exact energy of the Fermi level is, with respect to the most important interacting states, because that determines at what point this effect will start to diminish the Pauli repulsion. The very concept of "forbiddenness" of the depicted reaction has to be revised when the actual cause of the rise of the energy toward the barrier, which is the Pauli repulsion of the electrons in the occupied orbitals, is disappearing due to the escape route of the electrons toward the Fermi level. So this mechanism of softening of the Pauli repulsion may be expected to be the prime electronic structure reason for the unusual reactivity of (and at) metallic surfaces, and in a broad sense accounts for their versatility as heterogeneous catalysts.

This relief of the Pauli repulsion effect has been recognized before, but it has mostly been discussed only qualitatively. Post and Baerends[15−17] have tried to obtain some quantitative insight using the Morokuma-type of energy decomposition, where *A* was a CO molecule approaching the metal surface end-on (in which case *Ab* is the C lone pair orbital 5σ, and *Aa* is the CO 2π^*), and the metal was represented by clusters of various sizes. They noted the importance of relief of the Pauli repulsion by "configuration changes", which is the equivalent of the $(1a)^2 \rightarrow (2b)^2$ change noted above. In fact, the electronic configuration of the metal cluster can first be changed from $(Bb)^2 \rightarrow (Ba)^2$ so that the $(Ab)^2 - (Bb)^0$ orbital interaction becomes a donor−acceptor interaction and the $(Ba)^2 - (Aa)^0$ interaction becomes a back-donation (metal → adsorbate) interaction. These are both favorable, and replace the unfavorable $(Ab)^2 - (Bb)^2$ Pauli repulsion, at the cost, however, of the $(Bb)^2 \rightarrow (Ba)^2$ excitation energy. All of these energy terms can be quantified in cluster calculations.

We are not aware of other attempts to quantify by energy decomposition the particular electronic structure effect of the presence of a Fermi level. There are, however, qualitative discussions of the effect. The importance of emptying a metal−adsorbate antibonding level upon its crossing the Fermi energy has been stressed by Garfunkel and co-workers, both in the case of benzene chemisorption to a Rh surface[18] and in order to suggest a popssible activation barrier to chemisorption of CO to a Ni(111) surface.[19] We also mention the effect that CO adsorption may have on the surface magnetism, if the pushing above the Fermi level occurs for states of one spin but not the other (see Raatz and Salahub[20,21]). An interesting contribution was made by Harris and Andersson,[22] who compared the bond breaking of H_2 over a Cu_2 and a Ni_2 cluster. They chose precisely the atomic arrangement depicted in Figure 1, with atoms 3 and 4 the transition-metal atoms (Cu or Ni). In the case of Cu_2, assuming the Cu 4*s* atomic orbitals to be the only ones to play a role, the origin of the barrier for this reaction is exactly as described before for the $H_2 + M_2$ case, cf. Figure 1. However, in the case of Ni_2 they note that there are Ni 3*d* derived levels between the bonding and antibonding (mainly) 4*s* derived levels *Bb* and *Ba*. These are not fully occupied; there is an empty pair of antibonding 3*d*δ levels, which may be thought to define the Fermi energy in this case ("holes in the *d* band"), cf. Figure 2. The antibonding electrons in the 1*a* level

can be transferred to this 3*d* level, which accounts for lack of a barrier on the Ni surface. This model refers again to the Fermi sea acting as an electron sink, but it does not explain why in the case of Cu metal (as opposed to the Cu_2 cluster), the Fermi level that is also present in the Cu case, could not serve to receive the antibonding electrons out of the 1*a* level; such levels at the Fermi energy need not be *d* levels, *s*(*p*) levels may serve this purpose just as well.

A practical application of the importance of relief of Pauli repulsion by shedding antibonding electrons to the Fermi level has been noted in a study of the effect of subsurface O atoms upon the epoxidation catalysis by Ag surfaces. In this case, an incoming ethylene molecule reacts with an O atom residing on the Ag surface to form the ethylene oxide molecule. Subsurface O or Cl atoms have the effect of pushing up a crucial antibonding surface-O-ethylene π orbital, that would otherwise provide a barrier due to the Pauli repulsion it embodies, but that now ends up above the Fermi energy.[23] In the work of Hammer and Nørskov[24] on the reactivity of metallic surfaces, the notion of relief of Pauli repulsion when antibonding levels rise above the Fermi energy is a crucial element. They explain the lower bond energy of H atoms, and the higher barrier to H_2 dissociation, on group 11 metals (e.g., Cu) compared to 3*d* metals (e.g., Ni) by effects that follow from the difference in energetic position and occupation of the d bands in these metals, namely complete occupation of the 3*d* band in Cu, with the top of the d band being several electronvolts below the Fermi level, and a Fermi level that cuts through the top of the *d* band for Ni, that is, an incompletely occupied *d* band. The result should be less relief of Pauli repulsion in Cu because the antibonding 3*d* − H levels are mostly below the Fermi energy in Cu, but above it for Ni. Another effect will be the absence for Cu and presence for Ni of stabilizing empty 3*d* with occupied hydrogen orbital interaction (1*s* in atomic H, $1\sigma_g$ in H_2). Interestingly, the focus in their explanation is on the interaction with the *d* band, rather than with the *s* band, as was the case in Harris and Andersson's explanation.

Despite all of these qualitative discussions that have invoked the effect of relief of Pauli repulsion due to the presence of a Fermi surface, there is no quantification of the significance, if at all, of this effect. The closest to quantification are the energy decomposition calculations where the metal was represented with a cluster, but cluster models are quantitatively unreliable for chemisorption energy calculations precisely because the finite HOMO−LUMO gap in the cluster case cannot quantitively represent the relief of Pauli repulsion and the polarization of the metal, which both crucially depend on the presence of a Fermi level, that is, infinitely small gaps and a finite density of states around the energy E_F.[17,25]

We will in Section 2 of the present paper present a practical method for defining and calculating various energy terms in the decomposition of the chemisorption energy of a molecule on a metal surface. These terms are closely analogous to the ones that can be identified in interactions between molecular fragments. Their calculation, however, is more involved than that in the case of molecules, and we pay special attention to, for example, convergence with **k**-space integration. A key point is that we enrich the analysis with an extra term to capture the relief effect. Computational details are mentioned in Section 3. As illustrative applications, we consider in Section 4 two questions concerning metal−molecule interactions that have called for an explanation. We will apply our energy decomposition to the prototype problem of the barrier to H_2 dissociation on a coinage metal (Cu) versus its absence on a group 10 metal (Pd). But first we will consider the explanation for the fairly strong chemisorption bond of the notoriously unreactive N_2 molecule to the W(100) surface as an effect of relief of Pauli repulsion, as well as the existence of a barrier to molecular chemisorption in this case as a Pauli repulsion effect.

2. Fragment-Based Energy Analysis for Extended Systems

2.1. Bond Energy Decomposition. Let us first recapitulate the key elements of the fragment-based energy decomposition schemes commonly used to analyze the interaction between molecules with independent-electron methods such as Hartree−Fock and Kohn−Sham DFT. Although all of these methods do not define exactly the same number of terms, there is one concept that is shared by all. Central to the fragment analysis is constructing the antisymmetrized and renormalized product wave function, Ψ^0, from the fragment wave functions, see eq 1. In terms of the initial wave function, Ψ^0, the formation energy

$$\Delta E_{\text{bond}} = E_{\text{AB}} - E_{\text{A}} - E_{\text{B}} \tag{2}$$

is decomposed as

$$\Delta E_{\text{bond}} = \Delta E_{\text{prep}} + \Delta E^\circ + \Delta E_{\text{oi}} \tag{3}$$

The fragment preparation energy, ΔE_{prep}, is the energy required to change the geometry of the fragments to the geometry they obtain in the total system, without the other fragment being present. This term is, of course, always positive. The steric term is

$$\Delta E^\circ = E[\Psi^0] - \Delta E_{\text{prep}} - E_A - E_B \tag{4}$$

and the orbital interaction is

$$\Delta E_{\text{oi}} = E_{AB} - E[\Psi^0] \tag{5}$$

The wave function Ψ^0 is constructed according to eq 1 using antisymmetrization of fragment wave functions Ψ_A and Ψ_B, which are ground-state wave functions of the isolated fragments *in the final geometries*. The energy cost of going from optimized geometries to the final geometries in the isolated fragments is covered by ΔE_{prep}. Note that in this work we use the terms Pauli repulsion and steric repulsion interchangeably and somewhat loosely to refer to ΔE°, although it should be recognized that often the term Pauli repulsion is reserved for the part ΔE^{Pauli} of ΔE°, which remains after the classical electrostatic interaction ΔV_{elstat} (usually attractive) between the unmodified but interpenetrating electronic charge densities and nuclear charges of systems *A* and *B*, placed at their final positions, has been separated off: $\Delta E^\circ = \Delta E^{\text{Pauli}} + \Delta V_{\text{elstat}}$.[11]

The above procedure can be applied equally well to periodic systems. According to Bloch's theorem, the eigenfunctions of a Hamiltonian with a periodic potential can be chosen to be simultaneous eigenfunctions of the translation operators of the space group because the Hamiltonian commutes with these operators. The orbitals can be labeled accordingly $\psi_{n\mathbf{k}}$ with **k** being a continuous label corresponding to an irrep of the translation symmetry group. For any given **k** point, we have a set of occupied orbitals from fragments *A* and *B*, and we can proceed exactly as in the molecular case and mutually orthonormalize the occupied orbitals of fragments *A* and *B*. The **k** points are used in a **k**-space integration to obtain, for example, the density, ρ^0, corresponding to the wave function Ψ^0. The weights in that integration have been determined from our

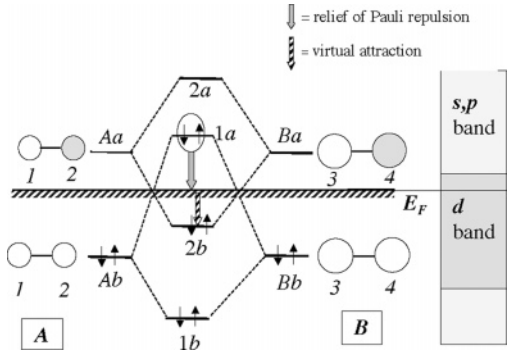

Figure 3. Relief of the Pauli repulsion embodied in the electron occupation of the antibonding level, by transfer of the electrons to the Fermi level, and virtual atraction by filling of a bonding combination of virtual orbitals that is stabilized below the Fermi level.

quadratic tetrahedron method.[26,27] They incorporate the weight function in the standard integration $\theta(E_F - \epsilon_{n\mathbf{k}})$, which ensures that the density is determined from the occupied states only. Although this procedure is straightforward, there is a numerical issue to be considered, which we relegate to the Appendix.

2.2. Modeling Relief of the Pauli Repulsion. Although it is of interest to evaluate the Pauli repulsion, we will demonstrate that it is the *relief* of this repulsion that is the crucial mechanism for a molecule−surface interaction. Before explaining how this can be modeled, let us first enumerate and describe the metal−molecule interactions as shown in the top panel of Figure 4. An interaction of class 1 between fully occupied orbitals is repulsive (contributes to the Pauli repulsion), and it can be relieved when its antibonding orbital like the 1*a* discussed before crosses the Fermi level. This is the relief mechanism as depicted in Figure 3. Interaction between empty orbitals (interaction 4) can also effect a configuration change: when its initially empty bonding combination (like the 2*b* orbital in Figure 3) drops below the Fermi level and becomes occupied, this interaction becomes bonding, otherwise it has no effect. We call this bonding mechanism *virtual attraction*. The virtual attraction and the relief of Pauli repulsion are both much more likely to occur for metal surfaces than for molecules. Then we have the commonly known charge transfer (or donor acceptor) orbital interactions 2 and 3, and the orbital interactions giving rise to internal polarization of the monomers, 5 and 6. All of these interactions have in common that they stabilize occupied orbitals and lift unoccupied ones, and hence do not lead to occupation change.

We use as our basis states the self-consistent orbitals of the fragments. One fragment is the metal slab used to describe the substrate, and the other fragment is the periodic overlayer of adsorbate molecules. These two systems are calculated with the same 2D unit cell size, using the same **k** points. With large surface unit cell size, so that the adsorbate molecules do not interact, the Bloch states at the **k** points can be formed immediately from the MOs of the adsorbate molecules. With this fragment basis, we can model the relief and virtual attraction contributions to the bonding energy by turning off interactions in the Fock matrix, analogous to the Morokuma method for intermolecular interactions. Starting from the sets of occupied orbitals o_A and o_B, and the virtual orbitals v_A and v_B, we first construct an orthonormal fragment basis by (Löwdin) orthonormalizing at each **k** point the occupied orbitals $o_A + o_B$, we next project out the occupied space from the virtual space and finally (Löwdin) orthonormalize the virtuals obtained after the projection. (With Löwdin orhonormalization, the resulting orbitals resemble the original ones as much as possible.[28]) In

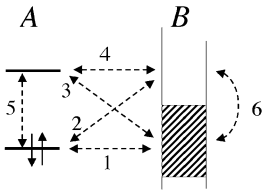

F	*Occ*(*A*)	*Occ*(*B*)	*Virt*(*A*)	*Virt*(*B*)
Occ(*A*)		Pauli Rep. (1)	Pol. (A) (5)	A→B (2)
Occ(*B*)	Pauli Rep. (1)		B→A (3)	Pol. (B) (6)
Virt(*A*)	Pol. (A) (5)	B→A (3)		Virtual Attr.(4)
Virt(*B*)	A→B (2)	Pol. (B) (6)	Virtual Attr. (4)	

Figure 4. Top: Types of interactions between a molecule and a metal. 1, occupied−occupied orbital interaction (Pauli repulsion); 2, molecule-to-metal donation interaction; 3, metal-to-molecule (back)donation interaction; 4, virtual attraction; 5, molecule polarization; 6, metal polarization. Bottom: Block structure of the Fock matrix (Kohn−Sham matrix) for interactions as labeled in the top panel at a given **k** point between the orbitals of the fragments *A* (molecule) and *B* (metal).

the orthogonalized fragment basis, the Fock matrix *F* (in our case the Kohn−Sham matrix) has the block structure shown in the bottom panel of Figure 4. In this basis we propose reduced matrices, shown in Figure 5. The first is $F^{(0)}$, which only uses the occupied−occupied block. Actually, a diagonalization is not necessary because it only produces a unitary tranformation of the orthogonalized occupied orbitals, which already give the energy of Ψ^0 because they define the density belonging to Ψ^0, as well as the kinetic energy, which are both invariant under further unitary transformation. Diagonalization may, of course, be performed in the restricted basis of occupied orbitals and would produce "canonical orbitals" with meaningful one-electron energies, in the field of the density ρ^0. The next step is to obtain the wave function Ψ^1 by performing a self-consistent calculation with on each cycle a diagonalization of the matrix $F^{(1)}$, see Figure 5. In this case, there are no interactions between occupied and virtual orbitals, and no interactions between the virtuals of one fragment with the virtuals of the other, but interaction between virtuals of the same fragment is retained. As a result, the total number of states that is included is the same as that in a full calculation, and complete bands of one-electron states are obtained. This affords the determination of a Fermi level in the usual way, by just filling up from below and fixing the Fermi level by the requirement that the correct total number of electrons is obtained by integration to the Fermi level. The energy $E[\Psi^1]$ incorporates the relief of the Pauli repulsion present in Ψ^0 because the electrons that were in high-lying antibonding states in the Ψ^0 step will now move down to states at the Fermi level. We define the energy difference

$$\Delta E^1_{\text{relief}} = E[\Psi^1] - E[\Psi^0] \tag{6}$$

as the relief of Pauli repulsion without virtual attraction because the interaction between virtuals of *A* and *B* is not allowed. We note that the definition of this energy term has a certain arbitrariness related to the choice of virtual space on *A* and *B*, respectively. The virtual spaces of *A* and *B* can each be made very large by adding more basis functions, until a complete basis set is reached. This would imply that, for instance, the occupied

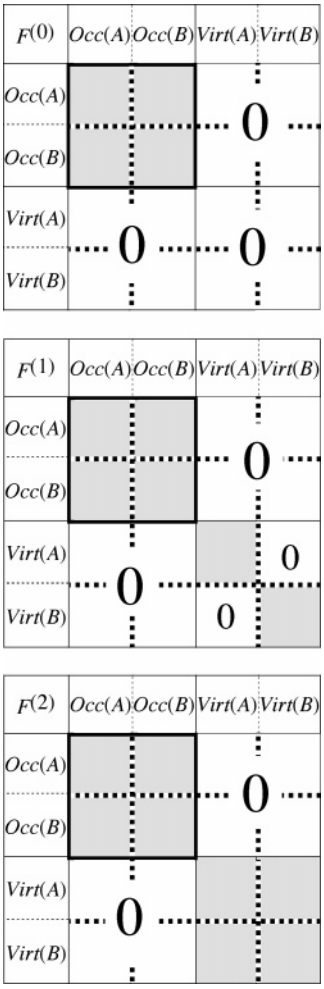

Figure 5. Reduced Kohn−Sham matrices. $F^{(0)}$ defines the Ψ^0 wave function with only occupied−occupied orbital interaction. $F^{(1)}$ and $F^{(2)}$ define the Ψ^1 and Ψ^2 wave functions, respectively; only the shaded part of the matrix is kept during the diagonalizations in the iterations to convergence.

plus virtual space of *A* incorporates the virtual space of *B*, so no virtuals on *B* can be allowed because overcompleteness would result. The virtual attraction, resulting from interaction of virtuals on *A* and *B* to be discussed shortly, would then already be obtained in this step. This is a somewhat formal objection; the basis sets on *A* and *B* in practice are far from complete and serve the purpose of representing decently the lower part of the virtual spectrum, the states at higher energies being very poorly described. But we do note that caution is to be exercised when interpreting the $\Delta E^1_{\text{relief}}$ values because they cannot be made to converge with basis set. It is therefore more rigorous to use the energy $E[\Psi^2]$ that is obtained by carrying out the self-consistent calculations with the Fock matrix $F^{(2)}$ of Figure 5, where interactions are fully allowed in the complete block of virtual levels of systems *A* and *B*. The energy

$$\Delta E^2_{\text{relief}} = E[\Psi^2] - E[\Psi^0] \tag{7}$$

has a proper basis-set limit and models the combined effect of the relief of the Pauli repulsion and the virtual attraction (the interaction of type 4). These are the only two occupation-changing interactions, which should be particularly effective for metals. The self-consistent procedures to obtain wave functions Ψ^1 and Ψ^2 can be applied equally well in calculations on finite systems (molecules). Because there is not a continuum of energy

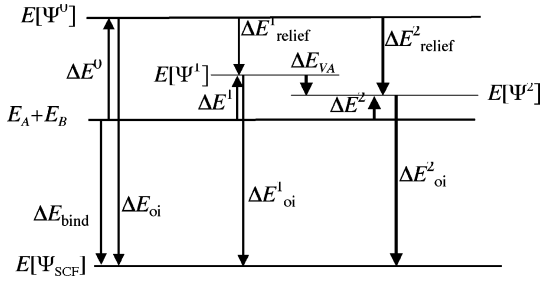

Figure 6. Overview of the various energy terms used in the energy decomposition, see the text. The preparation energy is assumed to be zero.

levels around the Fermi level in that case, one is then dealing with possible discrete configuration changes. For clusters, the importance of these discrete configuration changes, representing the relief of Pauli repulsion plus virtual attraction, has been stressed before.[17,25] Because of the variational principle we have $E[\Psi^2] \le E[\Psi^1]$ and hence (the relief terms are negative)

$$\Delta E^2_{\text{relief}} \le \Delta E^1_{\text{relief}} \tag{8}$$

2.3. Overview of Energy Terms. It is useful to generalize eq 4 and define three (relieved) steric terms for the three intermediate wave functions we have introduced for $i = 0, 1, 2$

$$\Delta E^i = E[\Psi^i] - \Delta E_{\text{prep}} - E_A - E_B \tag{9}$$

Here ΔE° is the original steric repulsion (eq 4), and ΔE^1 and ΔE^2 are relieved steric terms, corresponding to using either $F^{(1)}$ or $F^{(2)}$ in the self-consistent calculations. We finally note that a full self-consistent calculation, including the occupied−virtual orbital interactions of both charge-transfer type and polarization type, will afford the final converged total energy, $E[\Psi^{\text{SCF}}]$. This defines the orbital interaction energy term (eq 5) as

$$\Delta E_{\text{oi}} = E[\Psi^{\text{SCF}}] - E[\Psi^0] \tag{10}$$

Similarly, partial orbital interaction terms can be defined with respect to the energies $E[\Psi^1]$ and $E[\Psi^2]$

$$\Delta E^1_{\text{oi}} = E[\Psi^{\text{SCF}}] - E[\Psi^1] \tag{11}$$

and

$$\Delta E^2_{\text{oi}} = E[\Psi^{\text{SCF}}] - E[\Psi^2] \tag{12}$$

We display in Figure 6 the various energy levels we have defined and the corresponding energy differences. Note that the virtual attraction is defined as the difference between the energies of Ψ^2 and Ψ^1. Its definition is subject to the same objection regarding the basis-set dependence as the energy of Ψ^1 itself. We still feel that with the usual basis sets its magnitude should be a meaningful quantity, but we will obviously treat it with caution and in fact focus primarily on $\Delta E^2_{\text{relief}}$ as the defining quantity for the relief energy.

3. Computational Details

The calculations have been performed with the code BAND, which uses atom-centered basis functions, both Slater type orbitals, and numerical atomic orbitals.[29] We refer to refs 30 and 31 for recent discussions of details of convergence with basis set, with **k**-space integration, and with the real space numerical integration that is used in this code for the calculation

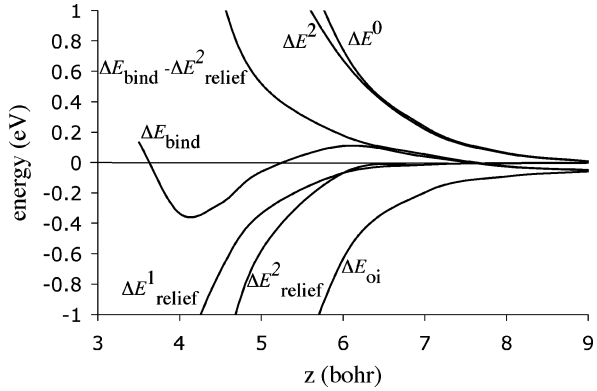

Figure 7. Energy decomposition terms for N_2 on W. Shown are the steric repulsion $\Delta E°$ (eq 4), the relieved steric repulsion ΔE^2 (eq 9), the relief energies ΔE^1_{relief} (eq 6) and ΔE^2_{relief} (eq 7), and the orbital interaction energy (eq 5). We have added $\Delta E_{bind} - \Delta E^2_{relief}$ to emphasize that there would be no binding without the relief term.

of the matrix elements of the Hamiltonian matrix. The calculations have been done within the generalized gradient approximation (GGA) of density functional theory. For H_2 on Cu and Pd, we have used the Becke Perdew (BP) functional,[32,33] and for N_2 on W we employed the RPBE functional[34] in order to be able to compare to the calculations performed by Serrano and Darling.[35] For all systems, the basis set was of "triple-ζ plus polarization" (TZP) quality, except for some of the convergence tests for the **k**-space integration, where we used a double-ζ plus polarization (DZP) basis, see the Appendix.

For all slab calculations, we have used two layers. The reason to do so is that the ultra dense **k**-space sampling that we need for the energy analysis prevents us from exploring thicker slabs. It should be realized that compared to the infinitely thick slab limit, the results differ typically ∼0.1 eV. For example, it has been shown[36] that for the chemisorption of H on Pd(111) the error is 0.05 eV. The calculated barrier of 0.79 eV for H_2 on Cu(100) in the TZP basis is 0.2 eV higher than the best known value (0.59 eV,[37] three layer slab) with the same (BP) functional. With the Perdew−Wang functional[38] we obtain a barrier of 0.67 eV, which differs only 0.1 eV from the 0.57 barrier obtained with a five-layer slab.[39]

4. Results

4.1. Chemisorption of N_2 to the Bridge Site on W(100); The Barrier to Chemisorption. Figure 7 shows how the energy decomposition terms develop for N_2 approaching end-on to a bridge site of a slab representing the W(100) surface. The bonding energy along this trajectory exhibits a small barrier (∼0.2 eV at 6 bohr) before a chemisorption well of 0.4 eV at 4 bohr, in agreement with Serrano and Darling.[35] (Their result was obtained with a five-layer slab, with the outermost two layers relaxed, and this confirms that our using two layers is a reasonable approximation.) Garfunkel and co-workers[18,19] have stressed that such barriers to chemisorption may arise from the Pauli repulsion between occupied levels. This is indeed entirely analogous to the way barriers arise in reactions between molecules. There has been a lingering doubt, however, because in this case, just as in "allowed" reactions, there will simultaneously be many possible occupied−virtual interactions. Hoffmann[13] expressed this doubt, commenting that "in reality, the repulsion at large metal adsorbate distances will be mitigated, and in some cases be overcome by attractive donor acceptor interactions". One might even go further and expect the (occupied−virtual) donor−acceptor term to start earlier than the (occupied−occupied) Pauli repulsion because of the larger spatial extent of virtual orbitals. Indeed, we see in Figure 7 that at very long distances, before the Pauli repulsion starts, the orbital interaction term already causes a (very weak) attraction: the bond energy is slightly negative (−0.03 eV) at our largest distance, 9 bohr. Serrano and Darling did not explore beyond 7 bohr and hence did not notice this weak attraction. Such a weak long-range attraction is not unusual in DFT calculations. The energy for H_2 over Pd(111), for example, is −0.05 eV (attractive) at 7 bohr when hydrogen (at the molecular equilibrium geometry) is perpendicular to the surface.[40] Our total energy decomposition shows unambiguously that the long-range attraction is caused by the total occupied−virtual term (donor−acceptor plus polarization), ΔE_{oi}, outweiging the Pauli repulsion, which is virtually negligible at such large distance. Purely virtual−virtual interactions play no role here because the relief term ΔE^2_{relief} is negligible beyond 6 bohr. The existence of this well is in agreement with the intuition that attractive occupied−virtual interactions have a longer range than the repulsive occupied−occupied interactions, but quantitatively the effect is very weak. Because we are in the distance range where van der Waals interaction will also play a role, which is not properly represented in the GGA functional, we should not expect quantitative accuracy of the depth of this small calculated potential energy well. We suspect that, more generally, for heterogeneous catalysis involving a metal surface the long-range interaction mechanisms are similar to those in homogeneous (gas phase) catalysis; a typical metallic feature such as the existence of a Fermi surface is not of special importance here. The extended nature of the surface is, of course, important for the long-range behavior, causing a slower decay of the van der Waals interaction.

At somewhat shorter distances, when the occupied−occupied overlap becomes significant, that is, below 7.5 bohr, the Pauli repulsion starts to outweigh the orbital interaction and the bond energy becomes repulsive. At still shorter distances, below 6 bohr, the relief sets in, and consequently ΔE^2 (and similarly ΔE^1, not shown) starts to become increasingly smaller than $\Delta E°$. Qualitatively, it appears that the increasingly negative ΔE^2_{relief} pulls the ΔE_{bond} curve down so that it first goes through a maximum and next even becomes attractive, forming a distinct chemisorption well. We also plot ΔE^1_{relief} and note the difference that develops with ΔE^2_{relief} suggests that the virtual attraction (cf. Figure 6) is indeed effective. But the virtual attraction contribution, although present, is not of major significance, so we will restrict ourselves to just the ΔE^2 and ΔE^2_{relief} terms. At very short metal−molecule distances, the bond energy curve rises again to build the repulsive wall, which, as always, is due to Pauli repulsion with lower-lying states (subvalence or semicore ones), see ref 11. We wish to stress that the relief of the Pauli repulsion due to the presence of a Fermi surface is indeed of crucial importance. The impact of the occupation-changing interactions is clearly borne out by the curve $\Delta E_{bond} - \Delta E^2_{relief}$: the bond energy in absence of the relief term is purely repulsive. This highlights the significance of the existence of energy bands and a Fermi surface. It is this essential electronic structure feature of a metal that gives rise to relief of the Pauli repulsion, hence bonding between the metal surface and the notoriously unreactive N_2 molecule. The essential point is that the relief energy is usually zero for gas-phase reactions because there is no band of energy levels around the Fermi energy to which antibonding electrons can escape. In a gas-phase "forbidden" reaction between molecules, occupation changes (changes of electronic configuration) will

TABLE 1: Energy Decomposition Terms for the Squeezing Together of Two Parallel Hydrogen Molecules, See Figure 1, at Distance *d* [a]

d (a_0)	ΔE_{bond}	ΔE^0	ΔE^2_{relief}	ΔE_{oi}
1.0	14.8	38.3	−18.3	−23.5
1.3	12.3	22.6	−6.6	−10.4
1.9	5.8	8.3	0	−2.4
2.5	2.3	3.0	0	−0.7
3.0	1.0	1.3	0	−0.2

[a] The hydrogen molecules are kept fixed at the gas-phase equilibrium geometry $r = 1.43a_0$

become effective in precluding further barrier rise only in extreme geometries, when the barrier has already been climbed rather far, that is, when it is already "too late". This stark contrast exposes the crucial role played by the Fermi surface.

To underline this marked difference, we have performed the energy analysis on the forbidden reaction of two hydrogen molecules approaching side-on as in Figure 1, keeping r at the equilibrium value and varying d, thus squeezing the molecules together. The bond energy, (see Table 1) is positive (repulsive) at all distances because the steric repulsion predominates over the orbital interaction. The repulsion grows continuously with decreasing distance d. The relief energy, as we indicated before, does not change in this gradual manner: it is exactly 0 for $d \geq 1.9$ bohr, the relief of the steric repulsion by configuration change only becoming active somewhere in the range $1.3 < d < 1.9$. At 1.9 bohr, the repulsion is already as much as 5.8 eV, the steric repulsion of 8.3 eV being only counteracted by a relatively small orbital interaction, because the 1*s*-derived σ_u cannot contribute, only high lying 2*s*- and 2*p*-derived levels can. The relief in this typical molecular case comes "too late" because the level 1*a* has to cross the large gap to 2*b*, see Figure 1. We note in passing that in the interval from 1.9 to 1.3 bohr we meet the situation that the system does not have an Aufbau solution with *integral* occupation numbers.[14] The exact density of the system in that distance region has to be represented by an ensemble, which effectively means that an Aufbau solution with *fractional* occupation numbers at the Fermi level should be obtained, which is possible, for example, with the technique of Averill and Painter.[41]

We end this section by noting that our present DFT results obtain a small barrier in the entrance channel for end-on approach of N_2 to the bridge site of W(100) and explain its origin. However, we cannot consider this a definitive demonstration that such a barrier exists. More extensive investigations (larger slab thicknesses, a range of functionals, or rather a more accurate electronic structure method than than GGA-DFT) would be required to prove its existence beyond any doubt. Regardless, however, of whether the occupied−occupied Pauli repulsion just tips the balance to repulsive bond energy, or just not, it is clear that this repulsive energy contribution is a significant factor in the shape of the potential energy surface even at a large distance such as 6 bohr.

4.2. Why is H_2 Dissociation an Activated Process on Cu and Not on Pd? In Figure 8 we present the energy terms for H_2 on Cu, and in Figure 9 we show the result for H_2 on Pd. We study dissociation of H_2 approaching parallel to the surface and dissociating over a bridge site, toward the neighboring hollow sites, cf. the inset in Figure 10. The H−H distance is denoted r, and the distance from the H_2 bond midpoint to the surface is denoted z. For the sake of comparison, the energies are plotted along exactly the same path in (z, r) space, namely along the intrinsic reaction coordinate for H_2 dissociation over the Cu(100) surface as depicted in Figure 10. The path is followed

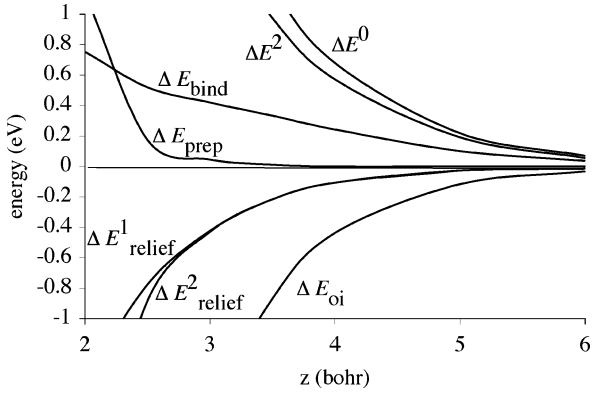

Figure 8. Energy analysis for H_2 on Cu, along the dissociation path, see Figure 10, to the hollow site over the bridge site. For a definition of the terms see Section 2.

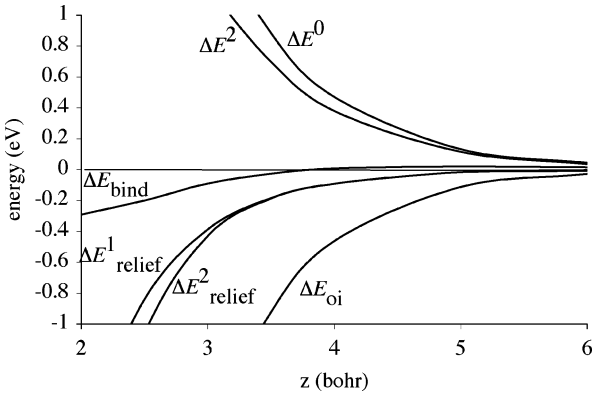

Figure 9. Energy analysis for H_2 on Pd. The reaction path is exactly the same as that for H_2 on Cu, see Figure 10. We have left out ΔE_{prep} because it is the same as that in Figure 8.

until the maximum of the barrier, which is at $z = 2.0$ bohr. Exactly the same path is used for the Pd case, which is fortunately pretty close to the intrinsic reaction coordinate in that case, as is evident from the corresponding PES in Figure 10. This is very helpful because ΔE_{prep} cancels in the comparison. The important difference between Cu and Pd is the purely repulsive bond energy curve in the case of Cu, representing the monotonic increase of the energy upon approach to the barrier. In the case of Pd, the bond energy is always negative, in agreement with the barrierless dissociation on this metal. We wish to understand the difference between these metals with the help of our energy decomposition. It is to be noted that in this case the distance between the H atoms varies along the reaction coordinate, that is, as a function of the z coordinate. This yields the additional ΔE_{prep} term in the total bonding energy ΔE_{bond}. It is only significant close to the barrier, where the H−H distance lengthens considerably. The other terms at a particular z are all calculated with respect to the H_2 molecule with the stretched bond length belonging to that point on the reaction path.

The behavior of the energy terms is superficially similar in the two cases (and similar to the N_2/W(100) case): With decreasing z we see growing positive steric terms ($\Delta E°$) and a growing negative total orbital interaction term ΔE_{oi}. The relief energy contributes to the total negative orbital interaction but clearly sets in at a relatively short range. The relief terms ΔE^1_{relief} and ΔE^2_{relief} hardly differ for $z \geq 3$ for both metals, and only little at shorter z, which means that virtual attraction does not play an important role in either case, and certainly not for the qualitative explanation of the differences between the metals.

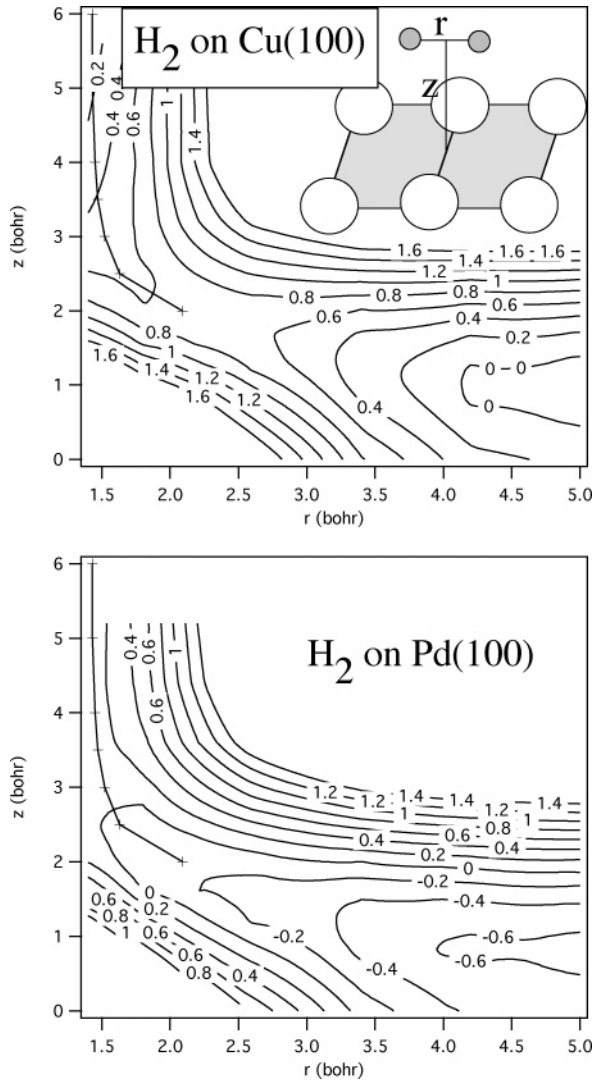

Figure 10. Potential energy surfaces for H_2 dissociation over bridge sites of Cu(100) and Pd(100). The intrinsic reaction coordinate of the Cu surface is also drawn in the Pd PES, and apparently coincides practically with the intrinsic reaction coordinate in that case.

Given this superficially similar behavior of the energy terms for the two metals, the important qualitative difference between these metals as dissociation catalysts must arise from seemingly subtle, yet important differences. To determine if the difference between the $\Delta E^2_{\text{relief}}$ terms, or indeed between one or both of the other terms, $\Delta E°$ and ΔE_{oi}, for the two metals, is the decisive factor for the difference in reactivity, we show in Figure 11 the differences in these energy terms. Note that $\Delta\Delta E°$ and $\Delta\Delta E_{\text{oi}}$ add up to the total difference in interaction energy $\Delta\Delta E_{\text{bond}}$, and $\Delta\Delta E^2_{\text{relief}}$ is part of the orbital interaction term. The differences are always taken as the energy term for H_2 on Cu minus the energy term for H_2 on Pd. All differences are positive, that is, less favorable for Cu, but obviously the crucial factor is the much stronger steric repulsion (Pauli repulsion) on Cu than on Pd. At the barrier ($z = 2.0$) it accounts for 70% of the total $\Delta\Delta E_{\text{bond}}$, and at larger distances this increases to even much higher percentages. The next important term is the $\Delta\Delta E_{\text{oi}}$. The least important is the difference in relief energies, $\Delta\Delta E^2_{\text{relief}}$. Our findings therefore do not confirm the interesting suggestion by Hammer and Nørskov[24,42] that the decisive difference, leading to a barrier in a noble metal like Cu, is the fact that the antibonding electrons between the H_2 σ_g orbital and the metal d states will still be below the Fermi energy, and therefore there

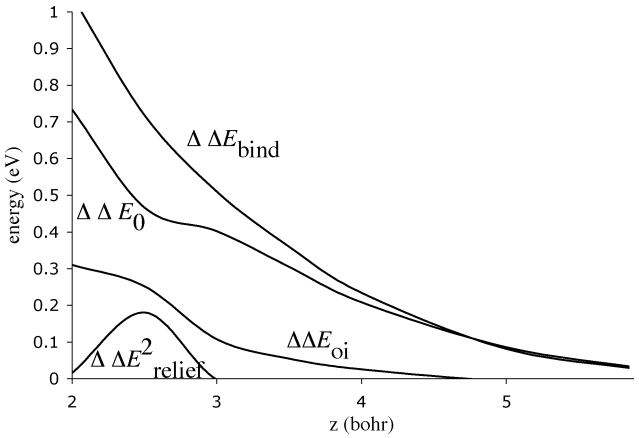

Figure 11. Energy differences between hydrogen on Cu and Pd. Shown are the difference in binding energy (eq 2), steric repulsion (eq 4), orbital interaction energy (eq 5), and relief energy (eq 7).

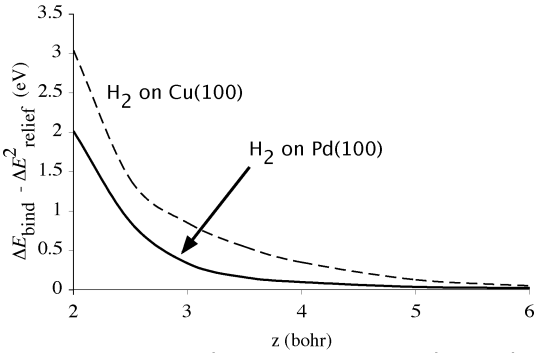

Figure 12. Bond energy curves along the reaction coordinate for H_2 on Cu(100) and H_2 on Pd(100) without the relief contribution $\Delta E^2_{\text{relief}}$.

cannot be a relief of this part of the Pauli repulsion, whereas in metals with the Fermi level in the *d* band, such as Pt and Pd, the antibonding states are pushed above the Fermi energy and such relief of the $d - \sigma_g$ Pauli repulsion *can* occur. We do find such a more favorable relief energy in Pd compared to Cu only at rather short *z*. However, the difference between the relief energies in Cu and Pd is at all distances quantitatively much smalller than the differences in the Pauli repulsion energies; it is only significant at $d \approx 2.5$, at $d \geq 3.0$, as well as at the barrier ($z = 2.0$) it is completely negligible. The orbital interaction, a negative (stabilizing) energy term, is stronger in Pd than in Cu, and this difference contributes to the lower (in fact nonexistent) barrier for Pd. In this case, the unfavorable effect of a higher repulsion energy for Cu is reinforced by a weaker orbital interaction energy. It is not usually the case that these energy contributions reinforce each other. It is more common, at least for molecules,[11] to find stronger repulsion being counteracted by (but usually not canceled by) stronger orbital interaction.

We finally wish to emphasize that the fact that we have found that the relief energy is not a distinguishing factor between Cu and Pd does not imply that the relief energy per se is not important for the reactivity of these metals. This is highlighted by showing, as we did for N_2 on W, the total bonding energy without the relief energy contribution $\Delta E^2_{\text{relief}}$, in Figure 12. It is clear that without the relief contribution the barrier in Cu would be much higher, and dissociation in Pd would no longer be barrierless, but meet the high barrier of 2.0 eV. This emphasizes the crucial role of the escape mechanism for antibonding electrons to the Fermi sea in relieving the Pauli repulsion with the occupied metal bands.

5. Conclusions

In conclusion, we have shown that it is feasible to adapt the energy decomposition analysis, which is well developed in the study of molecular interactions and reactions, to the realm of interactions of molecules with (metal) slabs. In particular, we have obtained for the first time, for three molecule−slab interactions, quantitative estimates of the steric (Pauli) repulsion, which has often featured in qualitative discussions of metal−molecule interactions in the past. Using an extension of the energy decomposition analysis for molecules, we have captured the effect of the abundance of states near the Fermi suface, in two "relief" energy terms. The first, $\Delta E^1_{\text{relief}}$, is the one closest to the intuitive relief of Pauli repulsion. The second, $\Delta E^2_{\text{relief}}$, incorporates the sometimes overlooked virtual attraction, and is unlike the previous term well defined in the basis-set limit. It can serve as a lower bound to the other term, see eq 8. We have employed these analysis tools to explain the existence of a clear chemisorbed state of N_2 approaching end-on a bridge site at the W(100) surface. The crucial factor appears to be the relief of the Pauli repulsion between the occupied N_2 orbitals and the occupied metal bands by antibonding electrons reverting to the Fermi level. The existence of a small barrier in front of the chemisorption well could be rationalized by this relief of the Pauli repulsion setting in only after the repulsive effects have started to build up.

When comparing the dissociation of H_2 over a Cu surface and a Pd surface, the analysis reveals that there is (considerably) more steric repulsion and (somewhat) less orbital interaction when hydrogen dissociates on the Cu surface, thus explaining why the process is activated on Cu and without barrier on Pd. Our picture differs from the one of Hammer and Nørskov[24,42] in that we do not attribute the difference between Cu and Pd to a smaller relief energy on Cu. As a matter of fact, our calculated relief energies do not differ much on Cu and Pd. By far the most important difference between these metals is the difference in Pauli repulsion energies. Although the difference in the relief energies of H_2/Cu and H_2/Pd is so slight, the absolute magnitude of the relief energy is quite significant in both cases. Without its presence, the dissociation over Pd would encounter a high barrier, and the barrier over Cu would be much higher still. This underlines the importance of this particular energy term to understand the way metals can act to bond to simple diatomic molecules such as N_2 and H_2 and in particular why they are so effective in lowering dissociation barriers. The existence of a Fermi level in a band of one-electron states is the crucial electronic structure feature that affords the relief mechanism. It makes the difference between heterogeneous (metallic) catalysis and homogeneous catalysis. It appears that only the metallic nature of the electronic structure, the very existence of a Fermi level in a band of one-electron states, is important. Two other properties of the electronic structure that have often entered discussions and modeling of metallic reactivity are a high density of states at the Fermi energy, and the presence of *d* holes. In the explanation for metallic reactivity that is proposed in this paper, we find no particular significance for these electronic structure features. Cu has a much lower density of states at the Fermi level than Pd, and has no *d* holes, yet can relieve the repulsion equally well.

Appendix: Brillouin Zone Integration

In a periodic calculation, the integrals over the Brillouin zone needed to calculate the total energy are of the form

$$I = \sum_n \int_{\text{BZ}} f_n(\mathbf{k})\Theta(E_{\text{F}} - \epsilon_n(\mathbf{k}))\, \mathrm{d}\mathbf{k} \qquad (13)$$

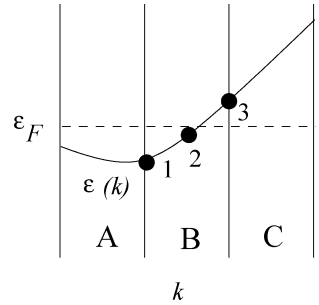

Figure 13. Integration in **k** space. Shown is a band of a fragment crossing the Fermi level of the fragment. The Brillouin zone is divided in three segments. In region A the band is unambiguously occupied, and in region C it is unoccupied. Only in the middle segment (B) the band is partly below and partly above the Fermi level. In case of analytic quadratic integration, the band is occupied in points 1 and 2 and unoccupied in integration point 3. The consequence of this discontinuity is that energy terms derived from Ψ^0 converge much slower than usual for the analytic method, see the text.

with band index n, property function $f_n(\mathbf{k})$, step function Θ, Fermi energy E_{F}, and dispersion $\epsilon_n(\mathbf{k})$. There are two orbital-dependent property functions that play a role in the evaluation of the total energy, namely the one for the density

$$f^{\rho}_n(\mathbf{k}) = |\psi_n(\mathbf{k})|^2 \qquad (14)$$

and the property function for the kinetic energy

$$f^{T}_n(\mathbf{k}) = -\frac{1}{2}\int_{uc} \psi_n(\mathbf{k},\mathbf{r})^*\nabla^2\psi_n(\mathbf{k},\mathbf{r})\, \mathrm{d}\mathbf{r} \qquad (15)$$

The discontinuous nature of the step function Θ makes the application of straighforward numerical integration to integrate eq 13 inefficient. In analytic schemes, the property function and the dispersion are interpolated by a polynomial in subregions of the Brillouin zone (tetrehedrons in the three-dimensional case, triangles in the two-dimensional case, simplices in general) or by periodic functions over the complete Brillouin zone (cf. the Monkhorst−Pack scheme). The integral is then evaluated exactly for the interpolated functions. We use quadratic interpolation in simplices (the quadratic tetrahedron method of refs 26 and 27), which converges relatively fast with the number of **k** points.

In the fragment analysis, we need integrals similar to eq 13 that are a sum over fragment terms (denoted by an index α)

$$I = \sum_\alpha \sum_n \int_{\text{BZ}} f^\alpha_n(\mathbf{k})\Theta(E^\alpha_{\text{F}} - \epsilon^\alpha_n(\mathbf{k}))\, \mathrm{d}\mathbf{k} \qquad (16)$$

but now the orbital-dependent property functions have discontinuities. Consider the interaction between two linear chains, where the **k** space is a line and the Brillouin zone a line segment. In our **k**-space integration technique, the "volume" (line segment) of the BZ is split up in a series of basic simplices (smaller line segments), in each of which the two **k** points at the end points and one in the middle is used to obtain second-order polynomial representations of both the dispersion relation $\epsilon_n(\mathbf{k})$ and the property function $f_n(\mathbf{k})$. Convergence can be obtained by making the simplices progressively smaller. Figure 13 shows the dispersion of a single band of a fragment crossing the Fermi level. In this example, the BZ is split into three segments, and in the leftmost segment the band is clearly occupied, and in the rightmost segment it is unoccupied. In the central segment, the band crosses the Fermi level so that in this segment the band changes from occupied to unoccupied. If we would use a quadratic integration scheme, where we interpolate

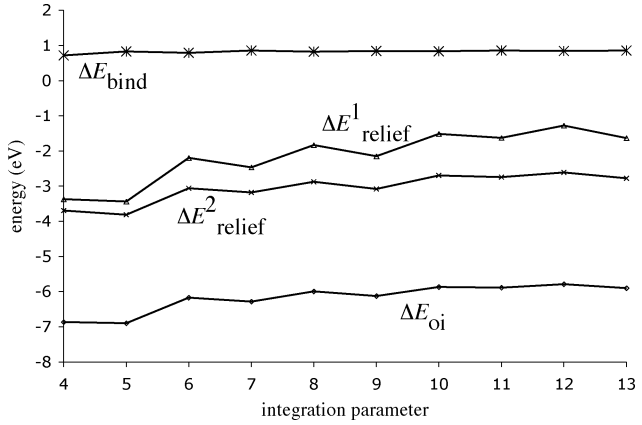

Figure 14. Convergence of the energy terms with respect to the **k**-space integration parameter, for H_2 on Cu(100) at the barrier geometry for bridge to hollow dissociation. These calculations have been performed with a smaller basis set of "double-ζ" quality, compared to the "triple-ζ" basis that was used in the final calculation.

the property function with a parabola, we would have three integration points (1, 2, and 3), shown as dots in the figure. In integration points 1 and 2 the band is occupied, and hence it is orthogonalized on the occupied orbitals of the other fragment, whereas in point 3 it is unoccupied and unchanged. So the value of for instance the property function $|\psi_n^{0,\alpha}(\mathbf{k},\mathbf{r})|^2$, which is the contribution to $\rho^0(\mathbf{r})$ from the Löwdin orthogonalized *n*th band ψ_n^α of fragment α, is not a smooth function of **k**. In this segment, property functions derived from the orbitals, like eqs 14 and 15, are not smooth. We will discuss elsewhere how the Brillouin zone integration can be adapted in order to deal with this specific problem, but in the present work we make use of the fact that the error can still be systematically reduced using an unmodified integration scheme by increasing the number of segments. Because certain conditions on the integrand (continuity of derivatives) are violated by the integrand in this case, we cannot expect the usual rapid convergence of the analytical BZ integration. We have tested the **k**-space integration convergence (in a DZP basis) of all energy terms for H_2 at the transition state for dissociation on the Cu(100) surface. Along the reaction path considered, it is here that all terms attain their maximum (absolute) value. The result for the convergence is shown in Figure 14. As can be seen, the bond energy converges much more quickly than the other terms. This is caused by the discontinuities of the orbital dependent property functions as explained above. For the bond energy the **k**-space integration parameter $K = 5$ (see refs 26 and 29) suffices, but because of the other terms we have settled for $K = 10$. The maximum variation in the energy terms for $10 \leq K \leq 13$ is 0.02 eV for ΔE_{bond}, 0.4 eV for $\Delta E^1_{\text{relief}}$, 0.06 eV for $\Delta E^2_{\text{relief}}$, 0.02 eV for ΔE_{oi}, so that only $\Delta E^1_{\text{relief}}$ is not entirely converged with this choice of integration parameter.

References and Notes

(1) Fleming, I. *Frontier Orbitals and Organic Chemical Reactions*; John Wiley and Sons: New York, 1976.
(2) Gimarc, B. *Molecular Structure and Bonding: The Qualitative Molecular Orbital Approach*; Academic Press: New York, 1979.
(3) Albright, T. A.; Burdett, J. K.; Whangbo, M. *Orbital Interactions in Chemistry*; John Wiley and Sons: New York, 1985.
(4) Burdett, J. K. *Theoretical Models of Inorganic Stereochemistry*; John Wiley and Sons: New York, 1980.
(5) Rauk, A. *Orbital Interaction Theory of Organic Chemistry*; John Wiley and Sons: New York, 1994.
(6) Jean, Y.; Volatron, F. *An Introduction to Molecular Orbitals*; Oxford University Press: New York, 1993.
(7) Morokuma, K. *J. Chem. Phys.* **1971**, *55*, 1236.
(8) Morokuma, K. *Acc. Chem. Res.* **1977**, *10*, 294.
(9) Kitaura, K.; Morokuma, K. *Int. J. Quantum Chem.* **1976**, *10*, 325.
(10) Weisskopf, V. W. *Science* **1975**, *187*, 365.
(11) Bickelhaupt, F. M.; Baerends, E. J. *Rev. Comput. Chem.* **2000**, *15*, 1.
(12) Burdett, J. K. *Chemical Bonding in Solids*; Oxford University Press: New York, 1995.
(13) Hoffmann, R. *Solids and Surfaces*; VCH: Weinheim (FRG), 1988.
(14) Schipper, P. R. T.; Gritsenko, O. V.; Baerends, E. J. *J. Chem. Phys.* **1999**, *111*, 4056.
(15) Post, D.; Baerends, E. J. *Surf. Sci.* **1981**, *109*, 167.
(16) Post, D.; Baerends, E. J. *Surf. Sci.* **1982**, *116*, 177.
(17) Post, D.; Baerends, E. J. *J. Chem. Phys.* **1983**, *78*, 5663.
(18) Garfunkel, E. L.; Minot, C.; Gavezotti, A.; Simonetta, M. *Surf. Sci.* **1986**, *167*, 177.
(19) Garfunkel, E. L.; Feng, X. *Surf. Sci.* **1986**, *176*, 445.
(20) Raatz, F.; Salahub, D. R. *Surf. Sci. Lett.* **1984**, *146*, 609.
(21) Raatz, F.; Salahub, D. R. *Int. J. Quantum Chem. Symp.* **1984**, *18*, 173.
(22) Harris, J.; Andersson, S. *Phys. Rev. Lett.* **1985**, *55*, 1583.
(23) van den Hoek, P. J.; Baerends, E. J.; van Santen, R. A. *J. Phys. Chem.* **1989**, *93*, 6469.
(24) Hammer, B.; Nørskov, J. K. *Nature* **1995**, *376*, 238.
(25) te Velde, G.; Baerends, E. J. *J. Chem. Phys.* **1993**, *177*, 399.
(26) Wiesenekker, G.; te Velde, G.; Baerends, E. J. *J. Phys. C: Solid State Phys.* **1988**, *21*, 4263.
(27) Wiesenekker, G.; Baerends, E. J. *J. Phys. Condens. Matter* **1991**, *3*, 6721.
(28) Mayer, I. *Int. J. Quantum Chem.* **2001**, *90*, 63.
(29) te Velde, G.; Baerends, E. J. *Phys. Rev. B* **1991**, *44*, 7888.
(30) Olsen, R. A.; Philipsen, P. H. T.; Baerends, E. J. *J. Chem. Phys.* **2003**, *119*, 4522.
(31) Fouquet, P.; Olsen, R. A.; Baerends, E. J. *J. Chem. Phys.* **2003**, *119*, 509.
(32) Becke, A. D. *Phys. Rev. A* **1998**, *38*, 3098.
(33) Perdew, J. P. *Phys. Rev. B* **1986**, *33*, 8822.
(34) Hammer, B.; Hansen, L. B.; Nørskov, J. K. *Phys. Rev. B* **1999**, *59*, 7413.
(35) Serrano, M.; Darling, G. R. *Surf. Sci.* **2003**, *532*, 206.
(36) Pallassana, V.; Neurock, M.; Hansen, L. B.; Hammer, B.; Nørskov, J. K. *Phys. Rev. B* **1999**, *60*, 6146.
(37) McCormack, D. A.; Kroes, G. J.; Olsen, R. A.; Baerends, E. J.; Mowrey, R. C. *J. Chem. Phys.* **1999**, *110*, 7008.
(38) Perdew, J. P.; Chevary, J. A.; Vosko, S. H.; Jackson, K. A.; Pederson, M. R.; Singh, D. J.; Fiolhais, C. *Phys, Rev. B* **1992**, *46*, 6671.
(39) Sakong, S.; Gross, A. *Surf. Sci.* **2003**, *525*, 107.
(40) Crespos, C.; Busnengo, H. F.; Dong, W.; Salin, A. *J. Chem. Phys.* **2001**, *114*, 10954.
(41) Averill, F. W.; Painter, G. S. *Phys. Rev. B* **1992**, *46*, 2498.
(42) Hammer, B.; Nørskov, J. K. *Surf. Sci.* **1995**, *343*, 211.